THE JOURNAL OF BIOLOGICAL CHEMISTRY VOL. 290, NO. 24, pp. 15175–15184, June 12, 2015

The Lipid Droplet Protein Hypoxia-inducible Gene 2 Promotes Hepatic Triglyceride Deposition by Inhibiting Lipolysis*

Received for publication, March 5, 2015, and in revised form, April 26, 2015 Published, JBC Papers in Press, April 28, 2015, DOI 10.1074/jbc.M115.650184

Marina T. DiStefano, Laura V. Danai, Rachel J. Roth Flach, Anil Chawla, David J. Pedersen, Adilson Guilherme, and Michael P. Czech[1]

From the Program in Molecular Medicine, University of Massachusetts Medical School, Worcester, Massachusetts 01605

Background: Excess hepatic triglyceride accumulation is associated with metabolic disease.
Results: Hig2 localizes to hepatic lipid droplets, enhancing their lipid content, and its deficiency increases triglyceride lipolysis.
Conclusion: Hig2 is a lipid droplet protein in hepatocytes that promotes liver triglyceride deposition by reducing its rate of degradation.
Significance: Hig2 is revealed as a critical lipid droplet protein controlling liver fat.

The liver is a major site of glucose, fatty acid, and triglyceride (TG) synthesis and serves as a major regulator of whole body nutrient homeostasis. Chronic exposure of humans or rodents to high-calorie diets promotes non-alcoholic fatty liver disease, characterized by neutral lipid accumulation in lipid droplets (LD) of hepatocytes. Here we show that the LD protein hypoxia-inducible gene 2 (*Hig2*/*Hilpda*) functions to enhance lipid accumulation in hepatocytes by attenuating TG hydrolysis. Hig2 expression increased in livers of mice on a high-fat diet and during fasting, two states associated with enhanced hepatic TG content. Hig2 expressed in primary mouse hepatocytes localized to LDs and promoted LD TG deposition in the presence of oleate. Conversely, tamoxifen-inducible Hig2 deletion reduced both TG content and LD size in primary hepatocytes from mice harboring floxed alleles of Hig2 and a cre/ERT2 transgene controlled by the ubiquitin C promoter. Hepatic TG was also decreased by liver-specific deletion of Hig2 in mice with floxed Hig2 expressing cre controlled by the albumin promoter. Importantly, we demonstrate that Hig2-deficient hepatocytes exhibit increased TG lipolysis, TG turnover, and fatty acid oxidation as compared with controls. Interestingly, mice with liver-specific Hig2 deletion also display improved glucose tolerance. Taken together, these data indicate that Hig2 plays a major role in promoting lipid sequestration within LDs in mouse hepatocytes through a mechanism that impairs TG degradation.

The liver is a major site of glucose, triglyceride (TG),[2] and fatty acid (FA) synthesis and serves as a master regulator of whole body nutrient homeostasis (1). Chronic exposure of humans or rodents to high-calorie diets can lead to a disease spectrum known as non-alcoholic fatty liver disease (2). This syndrome begins with simple neutral lipid accumulation in liver, progresses to liver inflammation, and can culminate in irreversible cirrhosis and hepatocellular carcinoma (3). Overabundance of liver lipids has also been associated with insulin resistance in both humans and rodents (4), although these conditions can also appear independently (5). Thus, understanding the molecular pathways that contribute to hepatic lipid accumulation is important in addressing therapeutic strategies for non-alcoholic fatty liver disease and in understanding how it relates to metabolic disease.

In all cells including hepatocytes, neutral lipids are stored in organelles termed lipid droplets (LDs) (6). These LDs are highly dynamic and are regulated by the nutritional status of the organism (7). Two main families of LD-associated proteins are the PAT family (7), named for its three founding members Perilipin, Adipophilin, and Tip47 that have PAT domains, and the cell death-inducing DNA fragmentation factor 45-like effector (CIDE) family (8). The PAT family has five members (Perilipin 1–5), whereas the CIDE family has three members (Cidea, Cideb, and Cidec/Fsp27). LDs are heterogeneous in their coats, and LD proteins generally demonstrate tissue-specific distribution patterns (9). In healthy murine liver, Perilipin 2 and Perilipin 3 promote LD formation (10), whereas Cideb promotes VLDL lipidation (11). Although deletion of Perilipin 3 has not yet been performed, genetic deletion of Perilipin 2 or Cideb ameliorates hepatic steatosis (12, 13). However, in the context of diet-induced obesity and fatty liver, Fsp27 (Cidec in humans) and Cidea are critical for LD formation (8). Both are highly up-regulated in murine liver upon diet-induced obesity, and genetic deletion of either also results in clearance of obesity-associated hepatic steatosis (8, 14, 15). Fsp27 is also relevant to human disease, as a patient with a homozygous nonsense mutation in *CIDEC* displays partial lipodystrophy, fatty liver, and metabolic syndrome (16, 17). As the proteome of the LD may be quite extensive (18), identifying additional members will shed new

* This work was supported by National Institutes of Health Grant R37-DK030898 (to M. P. C.).
[1] To whom correspondence should be addressed: Program in Molecular Medicine, University of Massachusetts Medical School, 373 Plantation St., Worcester, MA 01605. Tel.: 508-856-2254; Fax: 508-856-1617; E-mail: Michael.Czech@umassmed.edu.
[2] The abbreviations used are: TG, triglyceride; FA, fatty acid; LD, lipid droplet; CIDE, cell death-inducing DNA fragmentation factor 45-like effector; Hig2, hypoxia-inducible gene 2; HFD, high-fat diet; AV, adenovirus; Hig2iKO, Hig2-inducible knockout; Hig2LKO, Hig2 liver knockout; ND, normal diet; G0S2, G_0/G_1 switch protein 2; Ubc, ubiquitin C; qRT-PCR, quantitative RT-PCR; Tricine, *N*-[2-hydroxy-1,1-bis(hydroxymethyl)ethyl]glycine.

light on the mechanisms for TG deposition and potentially the basis of human disease.

Hypoxia-inducible gene 2 (*Hig2*/*Hilpda*) was initially identified in a screen for genes induced by oxygen deprivation in human cervical cancer cells and encodes a 7-kDa protein with little apparent homology to known proteins (19). Its expression is also increased in many cancers, particularly renal clear cell carcinoma, and it has been shown to be a target gene of both hypoxia-inducible factor 1 α (Hif1α) and peroxisome proliferator-activated receptor α (PPARα) (19–23). Gimm *et al.* (20) demonstrated that Hig2 localized to LDs and promoted TG deposition in cancer cells *in vitro*. These authors also showed that Hig2 co-localized with Perilipin 2 and 3, two LD proteins essential for neutral lipid deposition in healthy liver. Due to the importance of lipid homeostasis and deposition in liver, we examined the role of Hig2 in these processes.

Here, we demonstrate that Hig2 localizes to LDs in primary mouse hepatocytes. Importantly, its deletion in hepatocytes *in vivo* causes depletion of hepatic TG, indicating that it plays a physiological role in regulating liver lipid abundance in mice. Furthermore, we show that the basis for its ability to promote LD formation and TG deposition in liver is through the inhibition of TG lipolysis.

Experimental Procedures

Animal Studies

All of the studies performed were approved by the Institutional Animal Care and Use Committee (IACUC) of the University of Massachusetts Medical School. Animals were maintained in a 12-h light/dark cycle. Hig2$^{fl/fl}$ animals were purchased from The Jackson Laboratory (*Hilpdatm1.1Nat/J*). For metabolic studies, the animals were backcrossed onto C57Bl/6J animals for at least six generations. Genomic DNA was extracted from the obtained mice and subjected to PCR for genotyping using the Qiagen Fast Cycling PCR kit (Hig2$^{fl/fl}$ primer 5′-CCGGCAGGGCCTCCTCTTGCTCCTG-3′, 5′-GTGTGTTGGCTAGCTGACCCCTCGTG-3′). Hig2$^{fl/fl}$ animals were crossed to a tamoxifen-inducible ubiquitous cre mouse line (*B6.Cg-Tg(UBC-cre/ERT2)1Ejb/J*, The Jackson Laboratory). Hig2$^{fl/fl}$ animals were also crossed to an albumin cre mouse line (*C57BL/6-Tg(Alb-cre)21Mgn/J*, The Jackson Laboratory). Cre genotyping was performed according to the method of The Jackson Laboratory.

At 5–6 weeks of age, male C57Bl/6J, Hig2$^{fl/fl}$, or Hig2$^{fl/fl}$ albumin cre-positive littermates animals were placed on a high-fat diet (60% fat, 12492i Harlan) or fed chow (Lab Diet 5P76) for 12 or 16 weeks. Mice were fasted 16 h for glucose tolerance tests and 4 h for insulin tolerance tests. Mice were injected intraperitoneally with 1 g/kg of glucose or 1 IU/kg of insulin, blood was drawn from the tail vein at the indicated times, and blood glucose levels were measured with a Breeze-2-glucose meter (Bayer). Mice were euthanized by CO_2 inhalation followed by bilateral pneumothorax.

Plasma and Lipid Analysis

Mice were fasted for 3 h for plasma lipid analysis. Blood was taken via cardiac puncture, and EDTA-containing plasma was collected. Total serum cholesterol levels (ab65359 Abcam), serum triglyceride levels (triglyceride determination kit, Sigma), serum non-esterified fatty acids (Wako Diagnostics), and β-hydroxybutyrate (Sigma) were measured using calorimetric assays according to the manufacturer's instructions. Insulin levels were measured with an insulin ELISA Kit (Millipore) according to the manufacturer's instructions.

Triglyceride and Cholesterol Extraction

Whole livers were isolated and flash-frozen in liquid nitrogen. Lipids were extracted from livers or pelleted hepatocytes via the Folch method (24). Lipids were dissolved in isopropanol with 1% Triton X-100. Triglyceride (triglyceride determination kit, Sigma) and cholesteryl ester (ab65359 Abcam) levels were measured using calorimetric assays according to the manufacturer's instructions and normalized to liver weight or hepatocyte protein content.

Hepatocyte Isolation

Male or female 8–10-week-old chow-fed animals were anesthetized with an intraperitoneal injection of 1:1 ketamine:xylazine and perfused with Hanks' balanced salt solution supplemented with 0.5 M EGTA. Livers were digested with a perfusion of 50 mg/ml collagenase (Sigma, C6885) in Hanks' balanced salt solution supplemented with 1 mM $CaCl_2$, physically dissociated, and filtered through a 100-μm filter. Hepatocytes were washed, centrifuged at low speed, filtered through a 70-μm filter, and plated at a density of 1 million cells/ml.

RNA Isolation and RT-Quantitative PCR

Total RNA was isolated from cells or tissues using the TriPure isolation reagent (Roche Applied Science) according to the manufacturer's protocol. The isolated RNA was DNase-treated (DNA-free, Life Technologies), and cDNA was synthesized using the iScript cDNA synthesis kit (Bio-Rad). RT-quantitative PCR was performed on the Bio-Rad CFX97 using iQ SYBR Green supermix, and 36B4 served as the reference gene. Primer sequences are as follows: 36B4 (5′-TCCAGGCTTTGGGCATCA-3′, 5′-CTTTATCAGCTGCACATCACTCAGA-3′); Hig2 (5′-CATGTTGACCCTGCTTTCCAT-3′, 5′-GCTCTCCAGTAAGCCTCCCA-3′).

Immunoblotting

Tissues and cells were lysed in a high-salt, high-SDS buffer (2% SDS, 150 mM NaCl, 2 mM EDTA) with 1× Halt protease and phosphatase inhibitors (Thermo Scientific). Lysates were resolved by 15% SDS-PAGE gel run in a 1× Tris-Tricine buffer (National Diagnostics) and transferred to nitrocellulose membranes. Membranes were blotted with the following antibodies: β-actin (A2228, Sigma), HA-Tag (2367, Cell Signaling Technology). The Hig2 antibody was directed against a 15-amino acid peptide (PPKGLPDHPSRGVGV) at the C terminus of murine Hig2 (Rockland Immunochemicals).

Cell Culture

Hepatocytes were isolated from male or female 8–10-week-old Hig2$^{fl/fl}$ Ubc ERT2 cre-positive animals, plated in M199 adherence medium (Life Technologies, 11150, supplemented with 2% FBS, 10% BSA, 1% penicillin/streptomycin, 100 nM

insulin, and 100 nM dexamethasone) for 3 h, changed to M199 maintenance medium (M199 supplemented with 1% penicillin/streptomycin, 100 nM insulin, and 100 nM dexamethasone), and treated with ethanol vehicle or 2.5 μM (*Z*)4-hydroxytamoxifen (Sigma H7904) dissolved in filtered ethanol (5 mg/ml) for 48 h before experiments.

For imaging experiments, hepatocytes were plated on collagen-coated Millicell 4 chambered slides (Millipore) and transfected with GFP constructs using 1.5 μg of DNA, Opti-MEM, and Lipofectamine 2000 (Life Technologies) according to the manufacturer's instructions 48 h prior to experiments. Hepatocytes were also infected with HA-tagged adenoviruses 48 h prior to experiments. Cells were loaded with the indicated concentration of oleic acid (Sigma) dissolved in ethanol and conjugated to 10% fatty acid-free BSA dissolved in 0.1 M Tris pH 8. For radiation experiments, hepatocytes were plated on collagen-coated plates in William's E adherence medium (Life Technologies 12551, supplemented with 2% fetal bovine serum, 10% BSA (Sigma A4503), 1% penicillin/streptomycin, 100 nM insulin, and 100 nM dexamethasone). After 3 h, medium was changed to maintenance medium (William's E medium supplemented with 1% penicillin/streptomycin, 100 nM insulin, and 100 nM dexamethasone).

Cell Imaging

Cells were fixed in 10% buffered formalin in PBS for 15 min, stained with Oil Red O, and mounted with Prolong Gold with DAPI (Life Technologies). Cells were imaged at room temperature with a Solamere Technology Group modified Yokogawa CSU10 spinning disk confocal system with a Nikon TE-2000E2 inverted microscope at 60× and 100×. Images were acquired with MetaMorph Software, version 6.1 (Universal Imaging, Downingtown, PA).

Lipid droplet analysis was performed on fixed, Oil Red O- and DAPI-stained cells with BioPix iQ imaging software (BioPix AB, Göteborg, Sweden). At least 90 cells were analyzed per condition.

Oleate Tracer Studies

Hepatocytes were isolated from male 8–10-week-old $Hig2^{fl/fl}$ or $Hig2^{fl/fl}$ albumin cre-positive animals. 24 h after isolation, cells were loaded with 1 μCi/ml [^{3}H]oleic acid mixed with 100 μM oleic acid conjugated to 0.5% fatty acid-free BSA in William's E medium. Assays were performed as described previously (15, 25).

Oleate Uptake—Cells were loaded with 100 μM [^{3}H]oleic acid overnight. On the following day, medium was removed, cells were washed and lysed in 0.5 ml of lysis buffer (1% Triton-X100 in PBS), and lysates were placed in vials with scintillation fluid and counted using a Beckman LS 6500 scintillation counter. Counts were normalized to length of incubation time and protein content.

Total β-Oxidation—Cells were loaded with 100 μM [^{3}H]oleic acid overnight. On the following day, medium was collected, precipitated twice with perchloric acid and BSA, and spun to pellet insoluble products, and the soluble fraction was removed, placed in vials with scintillation fluid, and counted. Counts were normalized to length of incubation time and protein content. Empty medium was loaded with [^{3}H]oleic acid, precipitated, counted, and subtracted as a background reading.

Triglyceride Turnover—Cells were loaded with 100 μM [^{3}H]oleic acid overnight. On the following day, cells were washed two times, and medium was replaced with William's E medium with 0.6 mM triacsin C (Sigma). Cells were collected at the indicated times, washed, and lysed in 0.5 ml of lysis buffer (1% Triton X-100 in PBS), placed in vials with scintillation fluid, and counted. Counts are normalized to protein content and graphed as a percentage of time 0.

Lipolysis—Cells were loaded with 100 μM [^{3}H]oleic acid overnight. On the following day, cells were washed two times, and medium was replaced with William's E medium with 0.6 mM triacsin C (Sigma) and 100 μM etomoxir (Sigma). Medium was collected at the indicated times, placed in vials with scintillation fluid, and counted. Counts are normalized to protein content.

Statistical Analysis

Data were analyzed in GraphPad Prism 6 (GraphPad Software, Inc.). A two-tailed Student's *t* test with Welch's correction was used to compare two groups of data. Where indicated, data were analyzed using a two-way analysis of variance with repeated measures or a linear regression model. $p < 0.05$ was considered to be significant. The Grubb's test was used to determine whether there were statistical outliers, and if an outlier was determined, it was removed from the statistical analysis. Variance was estimated using S.E.

Results

To characterize Hig2 as a potential hepatic LD protein, we first determined whether it localized to LDs in primary mouse hepatocytes. We isolated primary hepatocytes from C57Bl/6J animals and transfected them with either GFP control or GFP-tagged Hig2 constructs and incubated them with oleic acid to induce LD formation. Although the GFP control construct displayed a diffuse, cytoplasmic distribution in the cells, the GFP-Hig2 construct clearly localized around the perimeter of Oil Red O-positive LDs (Fig. 1*B*). Gimm *et al.* (20) used deletion analysis to determine that the 37 N-terminal amino acids of Hig2 are required for LD targeting in cancer cell lines, which we termed the "putative lipid droplet binding domain" (Fig. 1*A*). To confirm that this was also the targeting domain in hepatocytes, we created a Hig2 truncation mutant with a loss of amino acids 1–28 of this putative binding domain. When the Hig2 truncation mutant was transfected into primary hepatocytes, it also localized diffusely, similar to the GFP control, demonstrating that Hig2 localizes to LDs in hepatocytes through this putative LD binding domain (Fig. 1*B*). As Gimm *et al.* (20) determined by sequence analysis that an amphipathic helix is located in this domain, it is possible that Hig2 may interact with the lipid droplet directly via surface interaction (26).

Hepatic LD protein expression is highly sensitive to nutritional status. As both Fsp27 and Cidea, two *bona fide* liver LD proteins, are highly up-regulated upon high-fat diet (HFD) feeding in mice (8), we measured Hig2 expression in two situations of hepatic steatosis. Fasting, which liberates lipids from adipose tissue via lipolysis, causes a temporary increase in liver

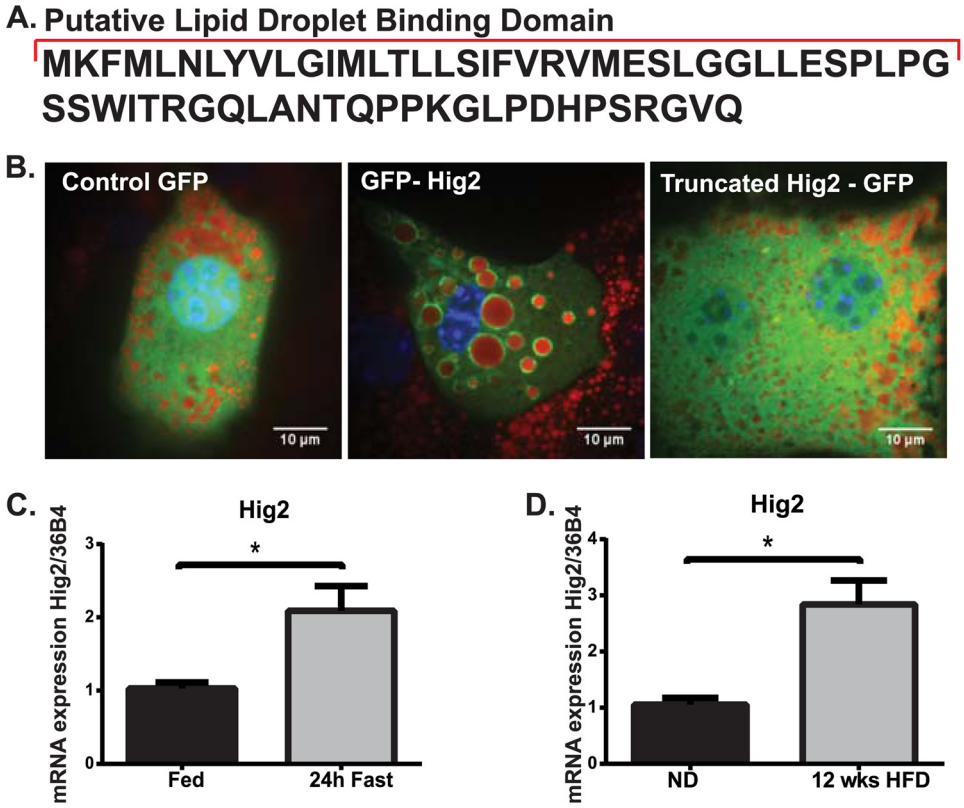

FIGURE 1. **Hig2 is localized to lipid droplets and is modified by nutritional status.** *A*, amino acid sequence of murine Hig2 with putative lipid droplet binding domain residues 1–37 indicated. *B*, hepatocytes were transfected with GFP-tagged constructs (*green*), loaded with 500 μM oleic acid for 4 h, fixed, and stained with Oil Red O (*red*) and DAPI (*blue*). Truncated Hig2-GFP is missing residues 1–28. *C* and *D*, whole livers were isolated from C57Bl/6J animals, RNA was extracted, and qRT-PCR was performed for Hig2 and normalized to 36B4. *C*, animals were fasted for 24 h or fed. Data are represented as the mean ± S.E. ($p < 0.05$, $n = 6$). *D*, animals were fed ND or HFD for 12 weeks. (*, $p < 0.05$, $n = 5–6$). Data are represented as the mean ± S.E.

lipids (27). Indeed, a 24-h fast caused a 2-fold increase in Hig2 mRNA expression in C57Bl/6J mouse livers (Fig. 1*C*). Obesity-induced hepatic steatosis in C57Bl/6J mice also caused a significant 2.7-fold increase in Hig2 mRNA expression in liver (Fig. 1*D*), consistent with the concept that Hig2 expression is highly correlated with liver lipid levels.

LD protein overexpression can also promote lipid deposition (7). For example, experimentally enhancing Fsp27 expression promotes TG accumulation in a variety of cell types, whereas Fsp27 deficiency reduces LD formation (28, 29). We tested whether Hig2 expression modifies TG accumulation in liver by manipulating Hig2 expression in primary mouse hepatocytes. First, we isolated primary hepatocytes from $Hig2^{fl/fl}$ animals and infected them with either control adenovirus (AV) or an AV expressing HA-tagged Hig2. As expected, Hig2-HA AV-infected cells demonstrated increased Hig2-HA levels as compared with controls as determined by Western blot (Fig. 2*B*). We incubated the cells with 250 μM oleic acid for 24 h to induce LD formation, fixed, and then stained them with Oil Red O to image LDs. Imaging revealed that Hig2-HA AV-infected hepatocytes had significantly more LDs as compared with controls (Fig. 2*A*). Although there was no significant difference in TG levels in BSA vehicle-treated hepatocytes, Hig2-infected cells demonstrated a 1.5-fold increase in TG content as compared with control cells after oleate loading (Fig. 2*C*). Taken together, these results demonstrate that high Hig2 expression is sufficient to promote lipid deposition in hepatocytes.

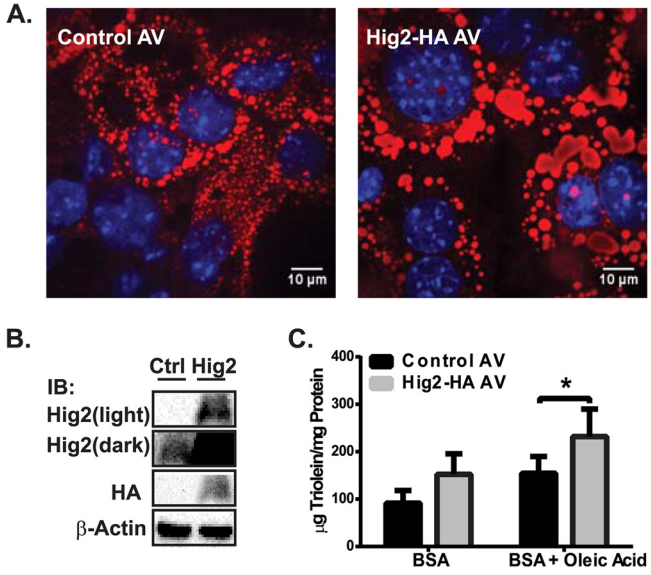

FIGURE 2. **Ectopic expression of Hig2 promotes hepatocyte lipid deposition.** Hepatocytes were isolated from $Hig2^{fl/fl}$ animals and infected with HA (control) or Hig2-HA (Hig2) adenovirus. *A* and *C*, hepatocytes were loaded with 250 μM oleic acid for 24 h. *A*, cells were fixed and stained with Oil red O (*red*) and DAPI (*blue*). *B*, representative immunoblots (*IB*) of Hig2 (light and dark exposure), HA-Tag, and β-actin. *Ctrl*, control. *C*, triglyceride content from control and Hig2-HA infected cells. (*, $p < 0.05$, $n = 6$). Data are represented as the mean ± S.E.

These results confirmed those of a study published while our studies were in progress showing that overexpression of Hig2 in liver via adeno-associated virus vector injection in

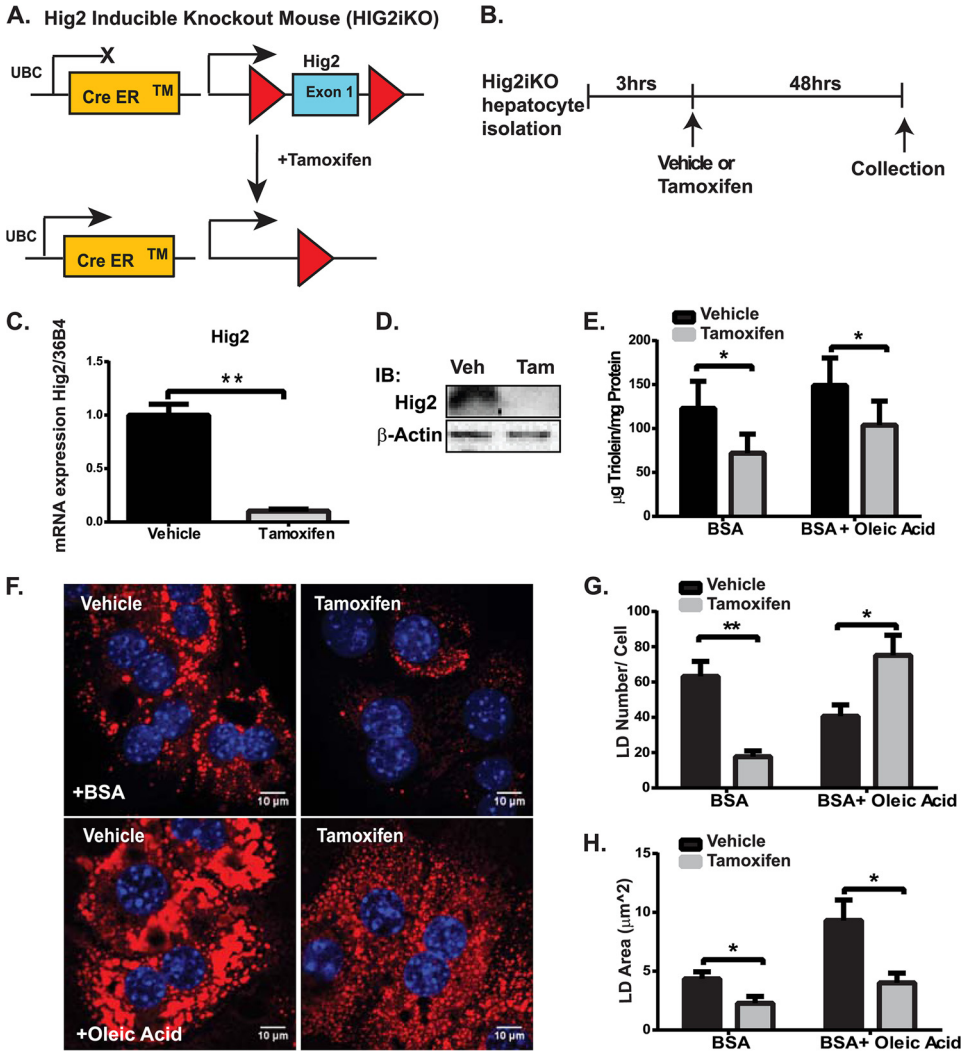

FIGURE 3. **Inducible Hig2 deficiency reduces lipid droplet triglyceride in hepatocytes.** *A*, schematic of Hig2 deletion with tamoxifen-inducible UbcERT2-cre. *B*, schematic of experimental design. Hepatocytes were isolated from Hig2iKO mice, plated for 3 h, and treated with ethanol vehicle or 2.5 μM tamoxifen in ethanol for 48 h. *C*, qRT-PCR was performed for Hig2 and normalized to 36B4. (**, $p < 0.01$, $n = 8$). *D*, representative immunoblots of Hig2 and β-actin. *IB*, immunoblot; *Veh*, vehicle; *Tam*, tamoxifen. *E*, triglyceride content from cells treated with 500 μM oleic acid or BSA vehicle for 4 h. *F*, hepatocytes were treated with BSA vehicle or 500 μM oleic acid for 24 h, fixed, and stained with Oil red O (*red*) and DAPI (*blue*). *G* and *H*, hepatocytes were treated with 500 μM oleic acid or BSA vehicle for 24 h. *G*, the number of lipid droplets per cell. *H*, total lipid droplet area per cell. (*, $p < 0.05$, **, $p < 0.01$, $n = 5–6$). Data are represented as the mean ± S.E.

mice resulted in increased hepatic lipid deposition *in vivo* (23).

Conversely, to determine whether Hig2 expression is necessary for lipid deposition in hepatocytes, we genetically deleted Hig2 in primary hepatocytes using a tamoxifen-inducible mouse model (Hig2iKO). We crossed Hig2$^{fl/fl}$ mice to Ubc ERT2 cre-positive mice (Fig. 3*A*), isolated hepatocytes from these Hig2iKO animals, plated them for 3 h, and treated them with either 2.5 μM 4-OH-tamoxifen to induce deletion or ethanol vehicle as a control for 48 h before analysis (Fig. 3*B*). Tamoxifen treatment resulted in a 90% reduction in Hig2 mRNA and protein expression as compared with ethanol vehicle-treated controls as assessed by qRT-PCR and Western blot, respectively (Fig. 3, *C* and *D*). Cells were fixed and stained with Oil Red O, and LDs were quantified. Strikingly, tamoxifen-treated hepatocytes had less Oil Red O-positive LD as compared with ethanol vehicle-treated controls (Fig. 3*F*). To confirm that this was not a side effect of tamoxifen treatment or the Ubc ERT2 cre transgene, we treated Hig2$^{fl/fl}$ or Ubc ERT2-positive hepatocytes on a wild type background with tamoxifen and observed no alterations in lipid accumulation (data not shown). When TG was extracted and quantified, we found that ethanol vehicle-treated cells had 1.7-fold more TG after BSA treatment and 1.4-fold more TG after oleic acid loading as compared with tamoxifen-treated cells (Fig. 3*E*). The ethanol vehicle-treated hepatocytes demonstrated an average of 63 ± 8 LD per cell, whereas tamoxifen-treated hepatocytes displayed over a 67% reduction in LD content and had an average of only 18 ± 3 LD per cell (Fig. 3*G*). Furthermore, the LDs in Hig2iKO hepatocytes were ~50% smaller than ethanol vehicle-treated controls and displayed an average size of 2.3 ± 0.6 μm^2 as compared with 4.3 ± 0.6 μm^2 for ethanol vehicle-treated controls (Fig. 3*H*). Interestingly, Hig2-deficient hepatocytes had significantly more LDs than controls after loading with 500 μM oleic acid for 24 h (41 ± 6 as compared with 75 ± 11); however, these LDs were over 50% smaller than control LDs (4.0 ± 0.8 μm^2

versus 9.3 ± 1.8 μm^2) (Fig. 3, *G* and *H*). This phenomenon is similar to the smaller LDs found in Fsp27-deficient adipocytes (29). These results demonstrate that Hig2 deficiency greatly reduced LD abundance and TG deposition in hepatocytes. Taken together, these experiments in primary hepatocytes suggest that Hig2 expression is required for hepatocyte lipid deposition and LD growth *in vitro*.

Excess accumulation of liver lipids is often associated with insulin resistance in obese mice and humans (4). Therefore, we generated mice with liver-specific deletion of Hig2 to address whether Hig2 deficiency could reduce hepatic steatosis and preserve glucose tolerance in a model of diet-induced obesity. We crossed the $Hig2^{fl/fl}$ mouse with mice expressing albumin cre to generate a mouse with liver-specific Hig2 deletion (Hig2LKO, Fig. 4*A*). Hig2LKO mice demonstrated a significant, 89% reduction of Hig2 mRNA specifically in hepatocytes as compared with fl/fl controls (Fig. 4*B*) and a concomitant reduction in Hig2 protein levels as determined by Western blot (Fig. 4*C*). Other tissues such as white adipose tissue, spleen, and kidney did not show significant reductions in Hig2 mRNA (Fig. 4*D*), demonstrating that the deletion was specific for hepatocytes. We placed these animals on HFD or normal diet (ND) for 16 weeks and measured their body weight weekly. Although there was no significant difference in the body weights of the Hig2LKO animals *versus* the fl/fl controls (Fig. 4*E*), the Hig2LKO animals demonstrated significantly improved glucose tolerance as measured by a glucose tolerance test both in the ND group and at early time points following glucose injection in the HFD-fed group (Fig. 4*F*). However, no significant difference between genotypes was observed in an insulin tolerance test (Fig. 4*G*).

We measured fasting circulating insulin levels, serum TGs, serum cholesterol, serum non-esterified fatty acids, β-hydroxybutyrate, and liver cholesterol, but all were unchanged among the groups in both the ND and the HFD-fed conditions (Table 1). Because Hig2 deletion reduces TG content *in vitro*, we examined the livers of the Hig2LKO animals fed ND or HFD for 16 weeks. The gross liver weights were not significantly different in either diet condition, but in the ND condition, the Hig2LKO animals had lighter livers than the fl/fl controls (1.14 ± 0.04 *versus* 1.23 ± 0.03 g, $p = 0.08$) (Fig. 4*H*). Although differences in H&E-stained histology sections from fl/fl and Hig2LKO animals were unremarkable (Fig. 4*J*), ND-fed Hig2LKO animals had 30% less liver TGs than fl/fl controls ($p = 0.08$); however, this difference was abrogated in HFD-fed animals (Fig. 4*I*). To assess liver inflammation, we isolated RNA from mice fed HFD for 16 weeks and performed qRT-PCR to assess the expression of genes involved in inflammatory pathways. No changes in gene expression were observed in Hig2LKO mouse livers as compared with fl/fl controls for *Tnfα*, *Il6*, *Il1β*, and the macrophage marker *Emr1* (F4/80) (data not shown).

We sought to examine potential mechanisms by which Hig2 controls TG accumulation in hepatocytes. Hepatic TG accumulation is controlled by FA uptake and hepatic lipogenesis *versus* hepatic lipolysis (TG turnover) (30). First, we performed qRT-PCR on RNA isolated from livers isolated from fl/fl and Hig2LKO mice on ND and assessed the expression of several genes that are critically involved in the aforementioned pathways. However, no changes in gene expression were observed in Hig2LKO mouse livers as compared with fl/fl controls for *Cd36* (FA uptake), *Cpt1a*, *Tfam* (mitochondrial oxidation), *Pparg*, *Fasn*, *Srebp1c* (lipogenesis), *Srebp2* (cholesterol synthesis), *Apob* (lipid export), or *Pnpla2* (Atgl) (lipolysis) (data not shown). Hig2 deficiency could potentially reduce the expression of other LD proteins in liver to reduce the lipid content. Thus, we also measured the expression of Perilipin 2 (*Plin2*), *Cidea*, and Fsp27 (*Cidec*) by qRT-PCR, and the expression of these genes was also unchanged in Hig2LKO mouse livers as compared with fl/fl livers (data not shown). Because there were no transcriptional changes in the targets we examined, we hypothesized that Hig2 was promoting hepatic lipid deposition in a post-transcriptional manner. Thus, lipid flux in Hig2LKO hepatocytes was assessed to determine whether they demonstrated a difference in lipid handling. We isolated hepatocytes from ND-fed fl/fl and Hig2LKO hepatocytes, incubated the cells with [^{3}H]oleic acid, and then measured the total amount of radiation in Hig2LKO and fl/fl controls after overnight [^{3}H]oleic acid loading. As expected, the Hig2LKO hepatocytes displayed a 45% reduction in lipid uptake as compared with controls ($p = 0.07$; Fig. 5*A*), confirming results obtained in Fig. 3 with the Hig2iKO hepatocytes.

Genetic deletion of LD proteins such as Fsp27, Perilipin 1, and Cidea in mice has demonstrated a role for LD proteins in TG turnover and β-oxidation (29, 31–33). Hepatic TG turnover has been experimentally determined to be on the timescale of 10–30 h *in vivo* (34). Thus, parameters were assessed by loading our ND-fed Hig2LKO or fl/fl hepatocytes with [^{3}H]oleic acid overnight, and then TG turnover, lipolysis, and β-oxidation were measured. Strikingly, despite the absence of changes in gene expression, Hig2LKO hepatocytes had significantly increased TG turnover as compared with fl/fl controls as determined by linear regression analysis (Fig. 5*C*). Hig2LKO hepatocytes also exhibited double the amount of lipolysis at 2 h as compared with controls (Fig. 5*D*). Similar to Fsp27-deficient animals, Hig2LKO hepatocytes also displayed 3.3-fold higher degree of FA oxidation as compared with control fl/fl hepatocytes as detected by accumulation of soluble [^{3}H]oleic acid oxidation products (Fig. 5*B*). Taken together, these results suggest that Hig2 promotes lipid deposition in a healthy liver, at least in part, by localizing to LDs in hepatocytes and inhibiting TG lipolysis.

Discussion

The findings presented here define Hig2 as a physiologically important LD-associated protein that functions to promote TG accumulation in liver *in vivo*. We demonstrated that GFP-tagged Hig2 localizes specifically to hepatocyte LDs in a manner that was dependent on its putative lipid binding domain (Fig. 1). Although ectopic expression of Hig2 promoted LD abundance and TG deposition (Fig. 2), Hig2 deletion in hepatocytes *in vitro* reduced TG accumulation (Fig. 3). Liver-specific Hig2 deletion reduced hepatic TGs in ND-fed mice and improved glucose tolerance in both the ND and the HFD-fed conditions (Fig. 4). Hepatocytes isolated from these animals show increased TG turnover and FA oxidation, suggesting that Hig2 promotes TG

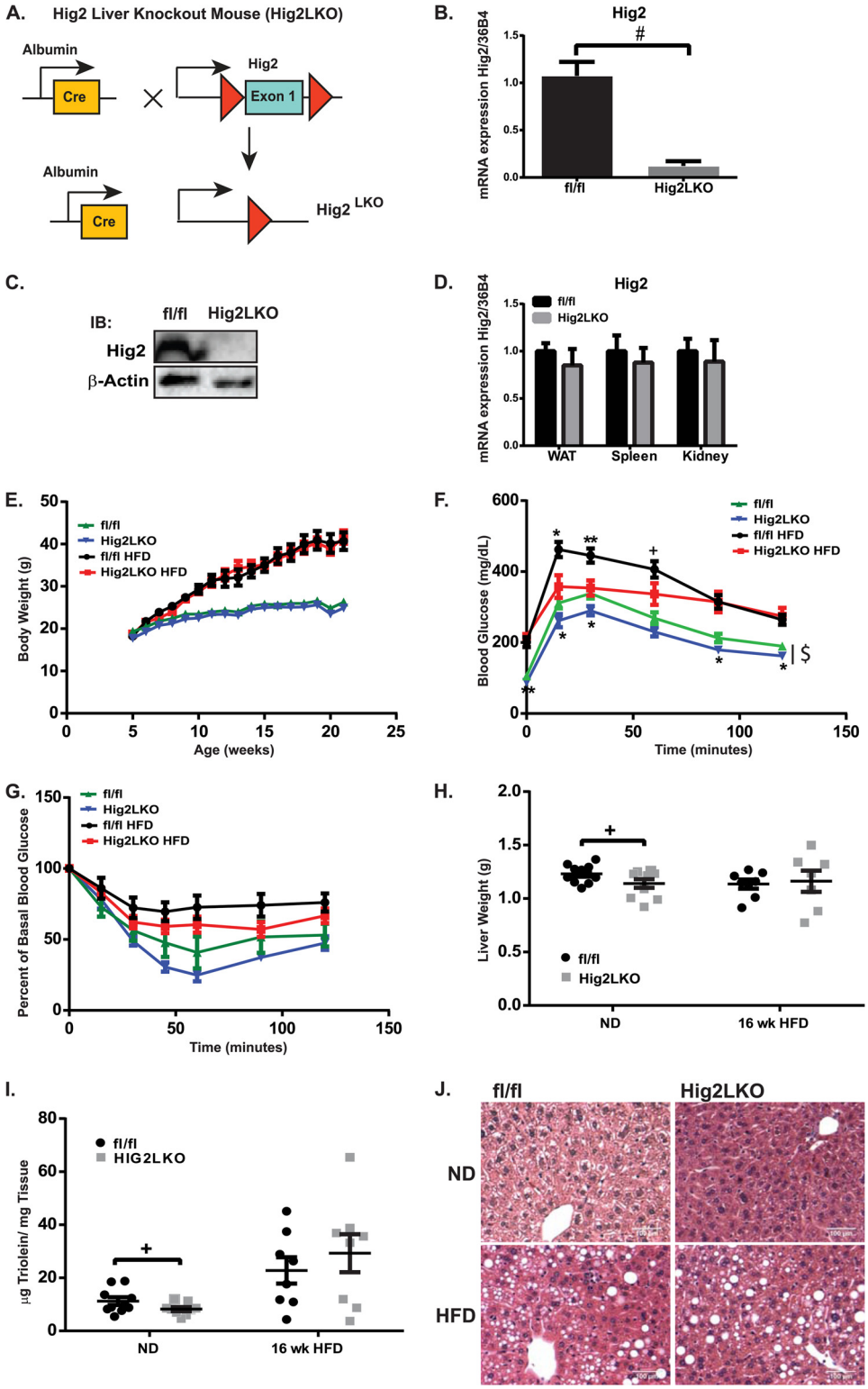

FIGURE 4. **Liver-specific Hig2-deficient mice display decreased liver triglyceride under normal diet conditions and improved glucose tolerance.** *A*, schematic of albumin-cre-mediated Hig2 deletion. *B* and *C*, hepatocytes were isolated from fl/fl and Hig2LKO mice. *B*, qRT-PCR was performed for Hig2 and normalized to 36B4. (#, $p < 0.005$, $n = 5$). Data are represented as the mean ± S.E. *C*, representative immunoblots (*IB*) of Hig2 and β-actin. *D*, white adipose tissue (*WAT*), kidney, and spleen were isolated from fl/fl and Hig2LKO mice. qRT-PCR was performed for Hig2 and normalized to 36B4. ($n = 8–9$). Data are represented as the mean ± S.E. *E–I*, fl/fl or Hig2LKO animals were fed ND or HFD for 16 weeks. *E*, body weight curves. ($n = 10–13$). *F*, glucose tolerance test. (+, $p = 0.08$, *, $p < 0.05$, **, $p < 0.01$; $, $p < 0.05$, two-way analysis of variance, $n = 7–11$). *G*, insulin tolerance test. ($n = 9–17$). Data are represented as the mean ± S.E. *H*, liver weights. (+ $p = 0.08$, $n = 8–11$). Data are represented as individual values ± S.E. *I*, lipids were extracted from livers, and triglyceride content was assessed. (+, $p = 0.08$, $n = 8–11$). Data are represented as individual values ± S.E. *J*, livers were sectioned and stained with H&E.

TABLE 1

Liver cholesterol and serum metabolites were assessed from fl/fl or Hig2LKO animals fed ND or HFD for 16 weeks

Data are the mean ± S.E. (n = 5–13). BD, below detection; NEFA, non-esterified fatty acids.

Parameters	Normal diet		16-week HFD	
	HIG2 fl/fl	HIG2LKO	HIG2 fl/fl	HIG2LKO
Insulin (ng/ml)	BD	BD	2.831 ± 0.477	2.640 ± 0.268
Serum triglycerides (mg/dl)	64.283 ± 4.302	51.456 ± 5.113	107.384 ± 6.634	102.954 ± 10.707
Serum cholesterol (mg/dl)	64.401 ± 5.782	70.218 ± 5.929	127.834 ± 6.993	137.622 ± 6.255
Liver cholesterol (μg/mg)	1.745 ± 0.106	1.717 ± 0.071	1.804 ± 0.226	2.181 ± 0.082
NEFA (mmol/liter)	0.416 ± 0.028	0.348 ± 0.038	0.536 ± 0.068	0.476 ± 0.058
β-Hydroxybutyrate (mmol/liter)	0.469 ± 0.042	0.569 ± 0.078	0.373 ± 0.038	0.274 ± 0.017

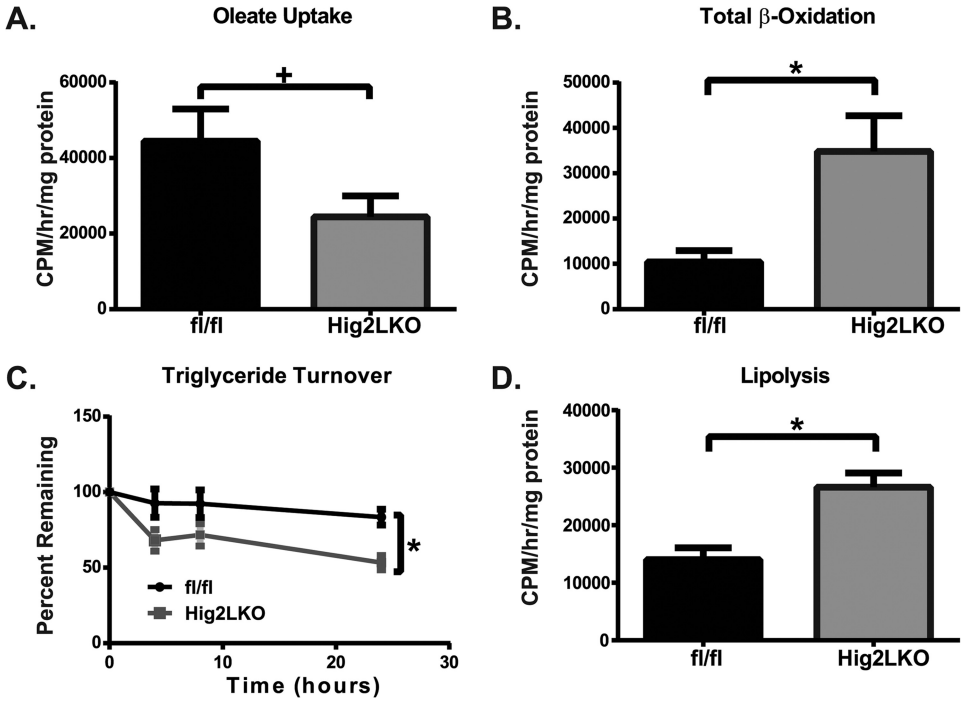

FIGURE 5. **Hig2 deficiency increases hepatocyte lipolysis, β-oxidation, and triglyceride turnover.** *A–D*, hepatocytes were isolated from fl/fl or Hig2LKO animals, plated, and loaded with 100 μM [^{3}H]oleic acid overnight. *A*, oleate uptake. (+, $p = 0.07$, $n = 8$). *B*, total β-oxidation. (*, $p < 0.05$, $n = 6$). *C*, triglyceride turnover. (*, $p = 0.05$ via linear regression analysis of the slope, $n = 8–10$). *D*, lipolysis. (*, $p < 0.05$, $n = 3$) Data are represented as the mean ± S.E.

deposition by inhibiting lipolysis (Fig. 5). Indeed, direct measurement of TG hydrolysis in hepatocytes deficient in Hig2 revealed increased lipolytic rates over controls, analogous to what has been reported for other LD proteins, such as Fsp27 (15).

As the data in Fig. 4 indicate, Hig2 may not be nearly as crucial for hepatic lipid deposition in HFD-fed liver as it is in the ND-fed condition. We found no decrease in total liver TG in the Hig2LKO mice as compared with fl/fl controls when both groups of mice were on an HFD. This contrasts with a decrease in liver TG observed in these Hig2LKO mice on ND (Fig. 4). One likely possibility to explain this result is other proteins that are redundant in function to Hig2.

Many LD proteins in the PAT family and the CIDE family have been shown to alter lipid deposition by inhibiting lipolysis (7, 8, 35). Some of these are up-regulated under HFD conditions and could replace Hig2 action on lipolysis. For example, it is well known that the expression of the LD protein Fsp27 is highly up-regulated under the fatty liver conditions we have examined here (36). Fsp27 was shown to inhibit lipolysis in adipocytes (28), similar to the present findings on Hig2 and hepatocytes. Taken together, it seems likely that compensation by other up-regulated LD proteins explains the failure of Hig2 depletion to lower liver TG under HFD conditions.

Our findings complement the recent findings of Mattijssen *et al.* (23) that were published while our studies were in progress. The authors demonstrated that overexpression of Hig2 in mouse livers driven by adeno-associated virus results in hepatic steatosis, similar to our results using AV as expression vector for Hig2 (Fig. 2). Consistent with their findings, we also observe increased lipid product export in hepatocytes from Hig2LKO mice as compared with controls (Fig. 5), but find that this export consists almost entirely of FA oxidation products rather than lipoproteins. It has been shown that increases in lipolysis can shunt FAs to the mitochondria, leading to increases in β-oxidation (37). We also observed that Hig2LKO hepatocytes had increased lipolysis and TG turnover, which is phenotypically similar to what is observed after loss of LD proteins and further suggests that Hig2 acts similarly to other proteins in this class. Thus, the increased β-oxidation products we observe in Hig2-deficient hepatocytes most likely reflects the higher levels of lipolysis and free FA availability for oxidation observed in the Hig2-deficient hepatocytes.

The increased lipolysis in Hig2LKO hepatocytes does not appear to be the result of altered expression of Atgl (data not shown), the rate-limiting TG lipase in adipose tissue. However, Atgl activity is known to be inhibited by G_0/G_1 switch protein 2 (G0S2) (38, 39). Hig2 could function similarly to negatively regulate lipolysis by interacting with and inhibiting Atgl or other lipases in liver. The lipolysis pathway in liver is not well studied, but liver-specific Atgl depletion in mice increases liver TG, whereas overexpression reduces liver TGs and increases β-oxidation independent of changes in hepatic gene expression or serum TGs, much like we observe in the Hig2LKO mouse (40–42). Sequence alignments of *Hig2* and *G0s2* show 13.5% sequence identity, mostly located in the area where G0S2 is known to bind and inhibit Atgl.[3] Another target of Hig2 regulation could be Adiponutrin, a lipase from the patatin-like phospholipase domain containing (PNPLA) family that contains the most sequence similarity to Atgl (37). If Hig2 physically interacts with a lipase, it could either inhibit its activity or restrict its access to LDs. The exact mechanism by which Hig2 inhibits lipolysis will be assessed in future studies.

A remarkable finding in this study was the significant improvement in glucose tolerance observed in liver-specific Hig2 deficiency, even under HFD conditions in which liver TG was unchanged (Fig. 4). Although in obese animals and humans liver TG accumulation generally correlates with insulin resistance, many experimental models show dissociation of liver lipid accumulation from glucose tolerance, and the precise mechanistic connections between liver fat and metabolism and insulin sensitivity are far from clear (5). The mechanism by which Hig2 improves glucose tolerance in HFD animals, primarily in early time points following glucose injection, is also unclear at this point. Hig2LKO animals trend toward enhanced insulin sensitivity in the insulin tolerance test (Fig. 4), although the differences did not reach statistical significance, and the basis of improved glucose clearance in these animals is under further investigation.

Although this work on Hig2 has been performed in murine cells and tissues, mutations in other LD proteins such as Fsp27 and Perilipin 1 are associated with human disease (16, 43). It will therefore be of interest to investigate whether Hig2 plays an important role in human biology. Tissue expression analysis of Hig2 shows that it is ubiquitously expressed.[3] This expression pattern parallels that of Perilipin 2, which can be found coating LDs in most tissues. This raises the question of whether Hig2 is required for lipid deposition in other tissues, particularly metabolically active tissues such as adipose tissue and muscle or for macrophage foam cell formation. The full range of Hig2 functions in diverse cell types in human biology is a key question for future research.

Acknowledgments—We thank Joseph Virbasius for critical reading of the manuscript and members of the Czech laboratory for helpful discussions.

[3] M. T. DiStefano, L. V. Danai, R. J. Roth Flach, A. Chawla, D. J. Pedersen, A. Guilherme, and M. P. Czech, unpublished observations.

References

1. Leavens, K. F., and Birnbaum, M. J. (2011) Insulin signaling to hepatic lipid metabolism in health and disease. *Crit. Rev. Biochem. Mol. Biol.* **46,** 200–215
2. Charlton, M. (2004) Nonalcoholic fatty liver disease: a review of current understanding and future impact. *Clin. Gastroenterol. Hepatol.* **2,** 1048–1058
3. Angulo, P. (2002) Nonalcoholic fatty liver disease. *N. Engl. J. Med.* **346,** 1221–1231
4. Birkenfeld, A. L., and Shulman, G. I. (2014) Nonalcoholic fatty liver disease, hepatic insulin resistance, and type 2 diabetes. *Hepatology* **59,** 713–723
5. Sun, Z., and Lazar, M. A. (2013) Dissociating fatty liver and diabetes. *Trends Endocrinol. Metab.* **24,** 4–12
6. Walther, T. C., and Farese, R. V., Jr. (2012) Lipid droplets and cellular lipid metabolism. *Annu. Rev. Biochem.* **81,** 687–714
7. Brasaemle, D. L. (2007) Thematic review series: adipocyte biology. The perilipin family of structural lipid droplet proteins: stabilization of lipid droplets and control of lipolysis. *J. Lipid Res.* **48,** 2547–2559
8. Xu, L., Zhou, L., and Li, P. (2012) CIDE proteins and lipid metabolism. *Arterioscler. Thromb. Vasc. Biol.* **32,** 1094–1098
9. Greenberg, A. S., Coleman, R. A., Kraemer, F. B., McManaman, J. L., Obin, M. S., Puri, V., Yan, Q. W., Miyoshi, H., and Mashek, D. G. (2011) The role of lipid droplets in metabolic disease in rodents and humans. *J. Clin. Invest.* **121,** 2102–2110
10. Patel, S., Yang, W., Kozusko, K., Saudek, V., and Savage, D. B. (2014) Perilipins 2 and 3 lack a carboxy-terminal domain present in perilipin 1 involved in sequestering ABHD5 and suppressing basal lipolysis. *Proc. Natl. Acad. Sci. U.S.A.* **111,** 9163–9168
11. Ye, J., Li, J. Z., Liu, Y., Li, X., Yang, T., Ma, X., Li, Q., Yao, Z., and Li, P. (2009) Cideb, an ER- and lipid droplet-associated protein, mediates VLDL lipidation and maturation by interacting with apolipoprotein B. *Cell Metab.* **9,** 177–190
12. McManaman, J. L., Bales, E. S., Orlicky, D. J., Jackman, M., MacLean, P. S., Cain, S., Crunk, A. E., Mansur, A., Graham, C. E., Bowman, T. A., and Greenberg, A. S. (2013) Perilipin-2-null mice are protected against diet-induced obesity, adipose inflammation, and fatty liver disease. *J. Lipid Res.* **54,** 1346–1359
13. Li, J. Z., Ye, J., Xue, B., Qi, J., Zhang, J., Zhou, Z., Li, Q., Wen, Z., and Li, P. (2007) Cideb regulates diet-induced obesity, liver steatosis, and insulin sensitivity by controlling lipogenesis and fatty acid oxidation. *Diabetes* **56,** 2523–2532
14. Zhou, L., Xu, L., Ye, J., Li, D., Wang, W., Li, X., Wu, L., Wang, H., Guan, F., and Li, P. (2012) Cidea promotes hepatic steatosis by sensing dietary fatty acids. *Hepatology* **56,** 95–107
15. Matsusue, K., Kusakabe, T., Noguchi, T., Takiguchi, S., Suzuki, T., Yamano, S., and Gonzalez, F. J. (2008) Hepatic steatosis in leptin-deficient mice is promoted by the PPARγ target gene *Fsp27*. *Cell Metab.* **7,** 302–311
16. Rubio-Cabezas, O., Puri, V., Murano, I., Saudek, V., Semple, R. K., Dash, S., Hyden, C. S., Bottomley, W., Vigouroux, C., Magré, J., Raymond-Barker, P., Murgatroyd, P. R., Chawla, A., Skepper, J. N., Chatterjee, V. K., Suliman, S., Patch, A. M., Agarwal, A. K., Garg, A., Barroso, I., Cinti, S., Czech, M. P., Argente, J., O'Rahilly, S., and Savage, D. B., and LD Screening Consortium (2009) Partial lipodystrophy and insulin resistant diabetes in a patient with a homozygous nonsense mutation in *CIDEC*. *EMBO Mol Med* **1,** 280–287
17. Zhou, L., Park, S. Y., Xu, L., Xia, X., Ye, J., Su, L., Jeong, K. H., Hur, J. H., Oh, H., Tamori, Y., Zingaretti, C. M., Cinti, S., Argente, J., Yu, M., Wu, L., Ju, S., Guan, F., Yang, H., Choi, C. S., Savage, D. B., and Li, P. (2015) Insulin resistance and white adipose tissue inflammation are uncoupled in energetically challenged Fsp27-deficient mice. *Nat. Commun.* **6,** 5949
18. Yang, L., Ding, Y., Chen, Y., Zhang, S., Huo, C., Wang, Y., Yu, J., Zhang, P., Na, H., Zhang, H., Ma, Y., and Liu, P. (2012) The proteomics of lipid droplets: structure, dynamics, and functions of the organelle conserved from bacteria to humans. *J. Lipid Res.* **53,** 1245–1253
19. Denko, N., Schindler, C., Koong, A., Laderoute, K., Green, C., and Giaccia, A. (2000) Epigenetic regulation of gene expression in cervical cancer cells by the tumor microenvironment. *Clin. Cancer Res.* **6,** 480–487

20. Gimm, T., Wiese, M., Teschemacher, B., Deggerich, A., Schödel, J., Knaup, K. X., Hackenbeck, T., Hellerbrand, C., Amann, K., Wiesener, M. S., Höning, S., Eckardt, K. U., and Warnecke, C. (2010) Hypoxia-inducible protein 2 is a novel lipid droplet protein and a specific target gene of hypoxia-inducible factor-1. *FASEB J.* **24,** 4443–4458
21. Nishimura, S., Tsuda, H., Nomura, H., Kataoka, F., Chiyoda, T., Tanaka, H., Tanaka, K., Susumu, N., and Aoki, D. (2011) Expression of hypoxia-inducible 2 (HIG2) protein in uterine cancer. *Eur. J. Gynaecol. Oncol.* **32,** 146–149
22. Togashi, A., Katagiri, T., Ashida, S., Fujioka, T., Maruyama, O., Wakumoto, Y., Sakamoto, Y., Fujime, M., Kawachi, Y., Shuin, T., and Nakamura, Y. (2005) Hypoxia-inducible protein 2 (HIG2), a novel diagnostic marker for renal cell carcinoma and potential target for molecular therapy. *Cancer Res.* **65,** 4817–4826
23. Mattijssen, F., Georgiadi, A., Andasarie, T., Szalowska, E., Zota, A., Krones-Herzig, A., Heier, C., Ratman, D., De Bosscher, K., Qi, L., Zechner, R., Herzig, S., and Kersten, S. (2014) Hypoxia-inducible lipid droplet-associated (HILPDA) is a novel peroxisome proliferator-activated receptor (PPAR) target involved in hepatic triglyceride secretion. *J. Biol. Chem.* **289,** 19279–19293
24. Folch, J., Lees, M., and Sloane Stanley, G. H. (1957) A simple method for the isolation and purification of total lipides from animal tissues. *J. Biol. Chem.* **226,** 497–509
25. Wang, H., Sreenivasan, U., Hu, H., Saladino, A., Polster, B. M., Lund, L. M., Gong, D. W., Stanley, W. C., and Sztalryd, C. (2011) Perilipin 5, a lipid droplet-associated protein, provides physical and metabolic linkage to mitochondria. *J. Lipid Res.* **52,** 2159–2168
26. Thiam, A. R., Farese, R. V., Jr., and Walther, T. C. (2013) The biophysics and cell biology of lipid droplets. *Nat. Rev. Mol. Cell Biol.* **14,** 775–786
27. Bechmann, L. P., Hannivoort, R. A., Gerken, G., Hotamisligil, G. S., Trauner, M., and Canbay, A. (2012) The interaction of hepatic lipid and glucose metabolism in liver diseases. *J. Hepatol.* **56,** 952–964
28. Puri, V., Konda, S., Ranjit, S., Aouadi, M., Chawla, A., Chouinard, M., Chakladar, A., and Czech, M. P. (2007) Fat-specific protein 27, a novel lipid droplet protein that enhances triglyceride storage. *J. Biol. Chem.* **282,** 34213–34218
29. Nishino, N., Tamori, Y., Tateya, S., Kawaguchi, T., Shibakusa, T., Mizunoya, W., Inoue, K., Kitazawa, R., Kitazawa, S., Matsuki, Y., Hiramatsu, R., Masubuchi, S., Omachi, A., Kimura, K., Saito, M., Amo, T., Ohta, S., Yamaguchi, T., Osumi, T., Cheng, J., Fujimoto, T., Nakao, H., Nakao, K., Aiba, A., Okamura, H., Fushiki, T., and Kasuga, M. (2008) FSP27 contributes to efficient energy storage in murine white adipocytes by promoting the formation of unilocular lipid droplets. *J. Clin. Invest.* **118,** 2808–2821
30. Nguyen, P., Leray, V., Diez, M., Serisier, S., Le Bloc'h, J., Siliart, B., and Dumon, H. (2008) Liver lipid metabolism. *J. Anim. Physiol. Anim. Nutr. (Berl.)* **92,** 272–283, 10.1111/j.1439–0396.2007.00752.x
31. Tansey, J. T., Sztalryd, C., Gruia-Gray, J., Roush, D. L., Zee, J. V., Gavrilova, O., Reitman, M. L., Deng, C. X., Li, C., Kimmel, A. R., and Londos, C. (2001) Perilipin ablation results in a lean mouse with aberrant adipocyte lipolysis, enhanced leptin production, and resistance to diet-induced obesity. *Proc. Natl. Acad. Sci. U.S.A.* **98,** 6494–6499
32. Zhou, Z., Yon Toh, S., Chen, Z., Guo, K., Ng, C. P., Ponniah, S., Lin, S. C., Hong, W., and Li, P. (2003) *Cidea*-deficient mice have lean phenotype and are resistant to obesity. *Nat. Genet.* **35,** 49–56, 10.1038/ng1225
33. Beylot, M., Neggazi, S., Hamlat, N., Langlois, D., and Forcheron, F. (2012) Perilipin 1 ablation in mice enhances lipid oxidation during exercise and does not impair exercise performance. *Metab. Clin. Exp.* **61,** 415–423
34. Tove, S. B., Andrews, J. S., Jr., and Lucas, H. L. (1956) Turnover of palmitic, stearic, and unsaturated fatty acids in rat liver. *J. Biol. Chem.* **218,** 275–281
35. Brasaemle, D. L., Rubin, B., Harten, I. A., Gruia-Gray, J., Kimmel, A. R., and Londos, C. (2000) Perilipin A increases triacylglycerol storage by decreasing the rate of triacylglycerol hydrolysis. *J. Biol. Chem.* **275,** 38486–38493
36. Aibara, D., Matsusue, K., Matsuo, K., Takiguchi, S., Gonzalez, F. J., and Yamano, S. (2013) Expression of hepatic fat-specific protein 27 depends on the specific etiology of fatty liver. *Biol. Pharm. Bull.* **36,** 1766–1772
37. Quiroga, A. D., and Lehner, R. (2012) Liver triacylglycerol lipases. *Biochim. Biophys. Acta* **1821,** 762–769
38. Lass, A., Zimmermann, R., Oberer, M., and Zechner, R. (2011) Lipolysis: a highly regulated multi-enzyme complex mediates the catabolism of cellular fat stores. *Prog. Lipid Res.* **50,** 14–27
39. Yang, X., Lu, X., Lombès, M., Rha, G. B., Chi, Y. I., Guerin, T. M., Smart, E. J., and Liu, J. (2010) The G_0/G_1 switch gene 2 regulates adipose lipolysis through association with adipose triglyceride lipase. *Cell Metab.* **11,** 194–205
40. Ong, K. T., Mashek, M. T., Bu, S. Y., Greenberg, A. S., and Mashek, D. G. (2011) Adipose triglyceride lipase is a major hepatic lipase that regulates triacylglycerol turnover and fatty acid signaling and partitioning. *Hepatology* **53,** 116–126
41. Reid, B. N., Ables, G. P., Otlivanchik, O. A., Schoiswohl, G., Zechner, R., Blaner, W. S., Goldberg, I. J., Schwabe, R. F., Chua, S. C., Jr., and Huang, L. S. (2008) Hepatic overexpression of hormone-sensitive lipase and adipose triglyceride lipase promotes fatty acid oxidation, stimulates direct release of free fatty acids, and ameliorates steatosis. *J. Biol. Chem.* **283,** 13087–13099
42. Wu, J. W., Wang, S. P., Alvarez, F., Casavant, S., Gauthier, N., Abed, L., Soni, K. G., Yang, G., and Mitchell, G. A. (2011) Deficiency of liver adipose triglyceride lipase in mice causes progressive hepatic steatosis. *Hepatology* **54,** 122–132
43. Gandotra, S., Lim, K., Girousse, A., Saudek, V., O'Rahilly, S., and Savage, D. B. (2011) Human frame shift mutations affecting the carboxyl terminus of perilipin increase lipolysis by failing to sequester the adipose triglyceride lipase (ATGL) coactivator AB-hydrolase-containing 5 (ABHD5). *J. Biol. Chem.* **286,** 34998–35006